

Improved emittance measurement system for the flat-beam experiment at FNPL

Y.-E Sun and P. Piot

June 14, 2005

Abstract

In this Note we discuss the modifications to the existing beamline of Fermilab/NICADD Photoinjector Laboratory (FNPL) in order to improve the flat-beam emittance measurement system. The slit-method is used for the measurement, and the corresponding apparatus includes beam viewers and masks with slit. We found that it is necessary to replace the existing multi-slit mask by single-slit masks due to the large emittance in the vertical plane. The distance between the slit and the beam viewer downstream is optimized for the measurement of both the large (in vertical plane) and small (in horizontal plane) emittance of the flat beam. We also present our study on the effect of the slit mask thickness. We found that it is advantageous to use a 2 mm thick slit mask comparing to 6 mm as of the multi-slit mask.

1 Introduction

Numerical simulations using Astra [1] are performed in order to study the flat-beam emittance measurement technique. A flat-beam with high emittance ratio is generated using the nominal parameters gathered in Table 1 ¹. The initial laser distribution is assumed to be radially uniform. A thermal emittance is included in the simulations by assigning a mean thermal energy of 0.75 eV to the photo-emitted electrons.

The evolution of beam rms emittance in the Larmor frame (i.e. the un-correlated beam emittance in laboratory frame) and the rms beam size from the photocathode to the entrance of the round-to-flat beam transformer channel is presented in Fig. 1.

From the beam phase-space distribution at $z = 3.77$ m generated numerically, we can estimate the two expected normalized flat-beam emittances as

$$\varepsilon_x = 0.11\text{mm mrad, and, } \varepsilon_y = 35.31\text{mm mrad,} \quad (1)$$

¹this machine set-up does not correspond to the nominal FNPL set-up. Our main goal here is to provide a more extreme case for the diagnostics simulations

parameter	value	units
laser injection phase	25	degree
laser radius on cathode	0.8	mm
laser pulse duration (Gaussian)	3	ps
bunch charge	0.5	nC
E_z on cathode	35	MV/m
B_0 on cathode	937	Gauss
booster cavity peak gradient	25	MV/m

Table 1: Settings for the photocathode drive laser, rf gun, and accelerating section.

which result in an emittance ratio around 300.

2 The round-to-flat beam transformation

The round-to-flat beam transformer consists of three properly tuned skew quadrupoles. The quadrupole locations in the beamline are: $z_1 = 4.020$ m, $z_2 = 4.371$ m, $z_3 = 5.224$ m.

From the simulated beam phase-space distribution at $z = 3.77$ m, the three skew quadrupole strengths are obtained using a MATLAB-based minimization algorithm, which uses as a starting point the analytical skew quadrupole strengths derived, under thin lens approximation, in Reference [2]. Two sets of solutions for the quadrupole strengths are obtained when the $x - y$ correlation is minimized at the exit of the transformer. For the nominal case (parameters in Table 1) we obtain for the normalized quadrupole strength (in the unit of $1/\text{m}^2$):

$$\begin{aligned} Q_k^1(1) &= -15.7837, & Q_k^1(2) &= +20.2479, & Q_k^1(3) &= -29.5653; \\ Q_k^2(1) &= +15.9793, & Q_k^2(2) &= -25.1088, & Q_k^2(3) &= -29.2920. \end{aligned} \quad (2)$$

The rms beam size and transverse emittance ratio along the beam line for the two sets of solutions (with 3D space charge on) are shown in Fig. 2 and Fig. 3.

3 Slit location and beamlet image downstream studies

At FNPL, under nominal operation, the space charge effects are important on the beam dynamics. Such effects prevent the use of standard envelope techniques (e.g. quadrupole scan) for measuring transverse emittance, and the slit method is used instead. For the sake of describing the slit-method, let's start with the rms envelope equation describing the

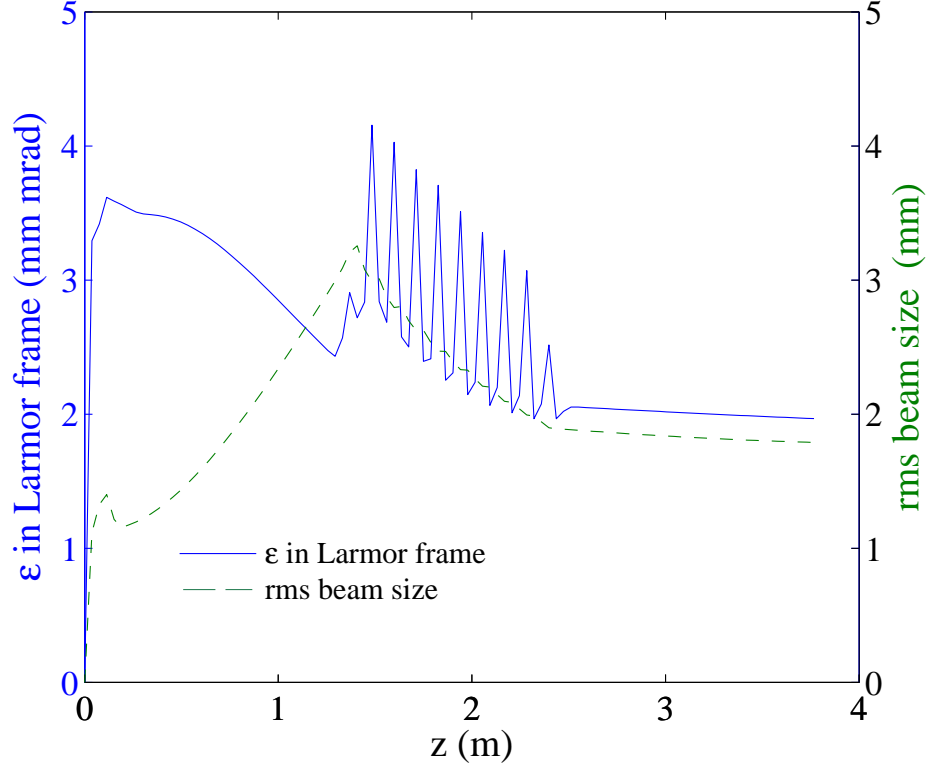


Figure 1: Beam emittance in Larmor frame and rms beam size before the skew quadrupoles.

evolution of a non-emittance-dominated beam in a drift space (from [3] p. 363):

$$\frac{d^2\sigma_x}{ds^2} = \frac{K}{2(\sigma_x + \sigma_y)} + \frac{\tilde{\varepsilon}_x^2}{\sigma_x^3}, \quad (3)$$

wherein $K \doteq (2I)/(I_0\beta\gamma^3)$ (from [3] p. 196) is the generalized perveance, $\sigma_{x,y}$ is the rms beam size and $\tilde{\varepsilon}_x$ the rms unnormalized emittance. The same type of equation is valid for y -plane by doing the transformation $x \leftrightarrow y$. If the beam is emittance-dominated, the emittance term in the latter equation must be the main contributor in the right-hand-side, i.e.:

$$R_x \doteq \frac{K\sigma_x^3}{2\tilde{\varepsilon}_x^2(\sigma_x + \sigma_y)} \ll 1. \quad (4)$$

In the case where the beam is collimated by some rectangular aperture with sizes w_x and w_y , we have:

$$\frac{Kw_x^3}{24\tilde{\varepsilon}_{x,C}^2(w_x + w_y)} \ll 1, \quad (5)$$

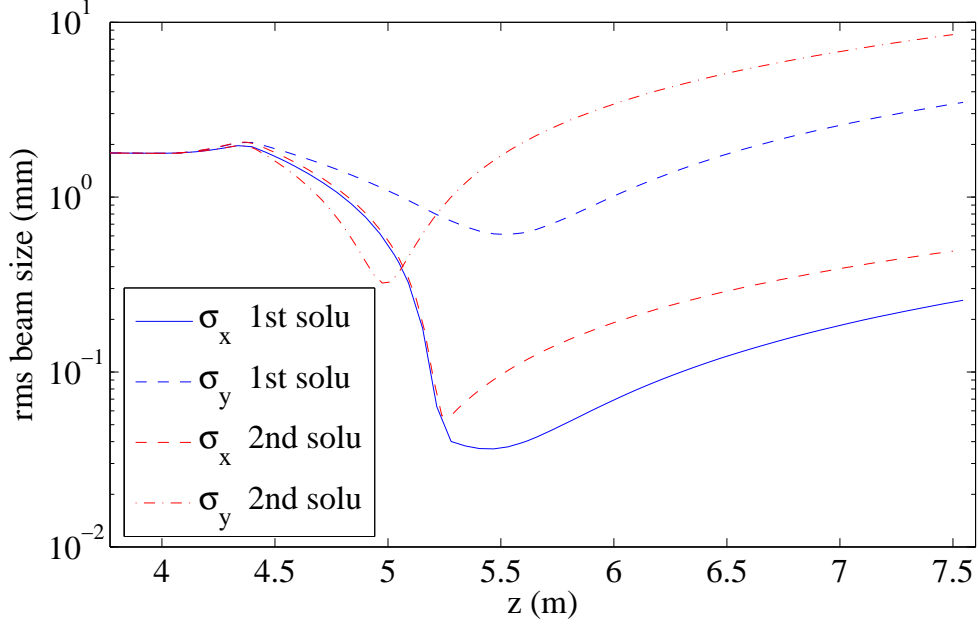


Figure 2: rms beam size during and after the skew quadruples.

where we replaced $\sigma_{x,y}$ by $w_{x,y}/\sqrt{12}$ in Eq. (4). Note that $\tilde{\varepsilon}_{x,C}$ is the emittance of the *collimated* beam. Substituting $\tilde{\varepsilon}_{x,C} = [w_x/(\sqrt{12}\sigma_x)]\tilde{\varepsilon}_x$ into Eq. (5), we have

$$\frac{Kw_x\sigma_x^2}{2\tilde{\varepsilon}_x^2(w_x + w_y)} \ll 1. \quad (6)$$

Let's consider a cylindrically symmetric beam which is intercepted by a multi-slit mask. From Eq. (4), upstream of the slit the space-charge over emittance ratio is (using the definition of R_x with $\sigma_x = \sigma_y$):

$$R_x = \frac{K\sigma_x^2}{4\tilde{\varepsilon}_x^2}. \quad (7)$$

downstream of the slits vertical slit of width w_x , we have:

$$\begin{aligned} \sigma_x &\rightarrow \zeta\sigma_x, \\ \sigma_y &= \sigma_x \text{ (the vertical beam spot is unchanged),} \\ K &\rightarrow \zeta K \text{ (because } I \rightarrow \zeta I), \\ \tilde{\varepsilon}_x &\rightarrow \zeta\tilde{\varepsilon}_x, \end{aligned}$$

where $\zeta \doteq w_x/(\sqrt{12}\sigma_x)$. The space-charge over emittance ratio thus becomes:

$$R'_x = \frac{K\zeta^4\sigma_x^3}{2\zeta^2\tilde{\varepsilon}_x^2(\zeta\sigma_x + \sigma_x)}. \quad (8)$$

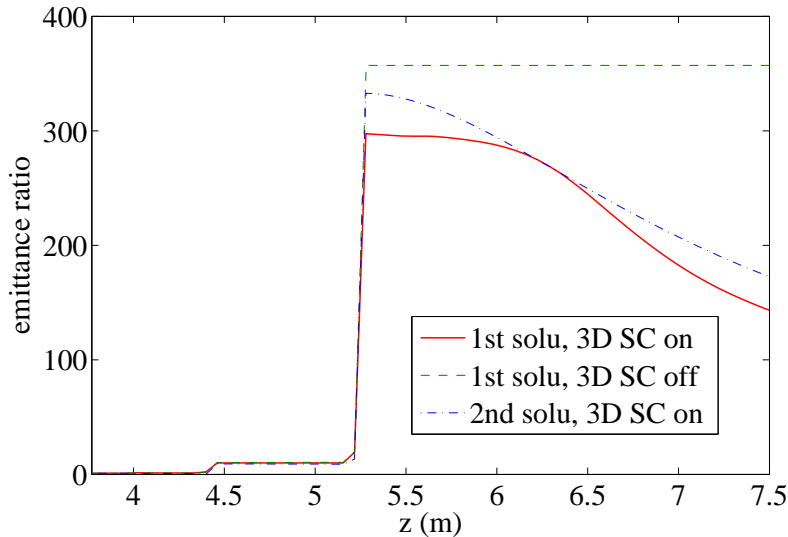


Figure 3: emittance ratio.

which yields under, under the assumption $\zeta \ll 1$:

$$R'_x \simeq \frac{K\zeta^2\sigma_x^3}{2\tilde{\varepsilon}_x^2\sigma_x} \simeq \frac{\zeta^2}{2} R_x. \quad (9)$$

At FNPL, we use the slit method to measure the beam emittances. At location $z = 5.62$ m, multislit tungsten plates are available in both the horizontal and vertical directions. The slit width is $50\mu\text{m}$, and the space between the center of two consecutive slits is 1 mm.

In the case of the flat beam generated using the parameters of Table 1, inserting such a horizontal multi-slits plate in the beamline and observing the beam on a downstream screen 40 cm away, we note that the correlation between a beamlet and the slit its generating slit has been lost: the beamlets are mixed; see Fig. 4. This renders the measurements of the rms sizes of each beamlet difficult. This observation suggests the use of a single movable horizontal slit which can be scanned vertically across the beam to sample different vertical locations. Examples of a horizontal slit inserted at the center and top of the beam are shown in Fig. 5 and Fig. 6.

Similarly, a single vertical a slit is used in order to measure the horizontal beam divergence; see Fig. 7 and Fig. 8.

4 Single beamlet rms size and beam emittance measurement

In order to decide the best location where to install a YAG screen to view the beamlet images, we track the beamlet in a drift downstream of the slit, with 3D space charge on. The rms size of the beamlets are computed from the particle distributions. The rms beam divergence σ'_x or σ'_y at the slit location are calculated via

$$\sigma'_x = \frac{\sqrt{(\sigma_x^V)^2 - \frac{w^2}{12}}}{z - z_0}, \quad (10)$$

$$\sigma'_y = \frac{\sqrt{(\sigma_y^H)^2 - \frac{w^2}{12}}}{z - z_0}, \quad (11)$$

where σ_x^V (σ_y^H) is the horizontal (vertical) rms size of the beamlet passing through a vertical (horizontal) slit, w the full width of the slit opening, z_0 the slit location along the beam line, and z the location where the beamlet image is observed (σ_x^V and σ_y^H are plotted in Fig. 9). We see that σ_y^H is growing quite fast. The YAG viewer has a diameter of ~ 2.5 cm, conservatively a beam with rms size less than 0.5 may be fully captured on the viewer. Considering also different initial beam conditions, we suggest that the YAG screen should be located approximately 80 cm downstream of the slit. In the example shown here, this corresponds to $\sigma_x^V = 70\mu\text{m}$, $\sigma_x^V = 1.2\text{mm}$. Given the camera calibration ($\approx 23\mu\text{m}$ per pixel), σ_x^V can be measured as well.

Finally the beam emittances inferred from the beamlet size measurements are shown in Fig. 10.

5 Effects of slits thickness

The nominal multi-slit mask used for the single shot transverse emittance measurement consists of series of tungsten segments (1 mm wide and 6 mm thick – the thickness the electron beam propagates through) stacked together with a spacer in between. The resulting assembly provides a series of 50 μm wide slits separated by 1 mm. For the single-slit assembly under consideration in this note, we reconsidered the required slit thickness (due to availability of 2 mm thick tungsten plate only). The slit samples in position the trace space of the beam and the fraction of the beam not going through the slit should be either stopped or scattered at large angle via multiple scattering. The rms angle of the scattered distribution, assumed to be Gaussian, is given by Molière theory [5]

$$\langle\theta^2\rangle^{1/2} = \frac{13.6[\text{MeV}]}{\beta cp} Z \sqrt{x/X_0} [1 + 0.038 \log(x/X_0)], \quad (12)$$

where p and Z are the particle incoming momentum and charge number, x is the particle path length in the material and X_0 is the radiation length of the material (3.5 mm for W [5]). Given the nominal operating energy of FNPL ($\beta cp \simeq 16$ MeV), a tungsten segment thickness of 2 mm yields a rms scattering angle of 0.63 rad. The latter rms scattering angle is much bigger than the angular acceptance determined by the downstream YaG viewer used to image the beamlet (we have $2 \text{ cm}/(80 \text{ cm}) \simeq 25 \text{ mrad}$). To further refine our study we used the computer program `shower` [6] which consists in an SDDS-compliant interface to the program EGS4 [7]. The flat distribution from astra at $z = 5.62$ m consisting of 500000 macro-particles was loaded into `shower` and tracking through an horizontal and vertical $50 \mu\text{m}$ wide slit in a 2 mm thick tungsten plate was performed. An histogram of the particle distribution, versus angle and energy, after passage through the slit mask is pictured in Figure 11. The beam distribution has large scattering angles beyond the acceptance of the beamline or the angular acceptance of the YaG screen. The corresponding transverse beam distribution obtained after tracking the phase space distribution at the slit mask exit up to the YaG screen, located 80 cm downstream, are shown in Figure 12. These images are simulations of the picture one would observed on the YaG screen including the resolution imposed by 768×1024 pixels CCD array of digital camera; the noise observed at large positions with respect to the beam core corresponds to electrons that have been scattered with a small angle (for instance partially going through the slit and hitting the slit edge).

In Table 2 we summarize the results of beam and beamlet spot sizes computed on the various distributions along with the estimated transverse emittances. Our calculation indicates that the retrieved emittance match the initial emittance computed on the incoming phase space distribution within 15% approximately.

In conclusion we have shown in this Section that a 2 mm thick tungsten plate can, in principle, be used for the single slit mask assembly. Reducing the plate thickness from 6 mm to 2 mm actually has the advantage of relaxing the angular alignment tolerance by a factor 3.

	$\sigma_{beam} (\mu\text{m})$	$\sigma_{beamlet} (\mu\text{m})$	$\sigma_{beamlet} (\mu\text{m})$	$\tilde{\epsilon}_{ret} (\text{mm-rad})$	$\tilde{\epsilon}_{ini} (\text{mm-rad})$
hor.	40.5	—	78.2	0.14	0.12
ver.	633.9	1484.7	—	40.97	35.28

Table 2: Summary of beam (σ_{beam}) and beamlet ($\sigma_{beamlet}$) transverse dimensions along with retrieved emittance $\tilde{\epsilon}_{ret} \doteq \gamma\sigma_{beamlet}\sigma_{beam}/L$ compared with nominal emittance computed on the initial phase space ($\tilde{\epsilon}_{ini}$).

6 conclusion

A single horizontal or vertical slit would be helpful to improve the emittance measurement of a flat beam. A YAG screen located 80 cm downstream of the slit is a good compromise between trying to catch all of the horizontal beamlet image (whose rms in y grows rapidly) and get enough resolution of the vertical beamlet image. The experimental set-up presented in this Note was implemented in FNPL, and led to the measurement of flat beam with transverse emittance ratio of 100 [8].

References

- [1] K. Flöttmann, “ASTRA: A Space Charge Tracking Algorithm”, user manual available at http://www.desy.de/~mpyflo/Astra_dokumentation.
- [2] E. Thrane *et al.*, in *Proceedings of the XXI International Linac Conference, Gyeongju, Korea* (Pohang Accelerator Laboratory, Pohang, Korea, 2002), pp. 308-310.
- [3] M. Reiser, “Theory and Design of Charged Particle Beams”, John Wiley & Sons, INC. (1994).
- [4] P. Piot and Y.-E Sun, Fermilab Beams Document 1346-v1.
- [5] Review of Particle Physics, Euro Phys. Jour. **C 3**, num 1-4 (1998) pg. 146
- [6] L. Emery, *User’s Guide to shower version 1.0, an EGS4 Interface* available at http://www.aps.anl.gov/asd/oag/manuals/shower_V1.0/shower.pdf.
- [7] W. R. Nelson, H. Hirayama, and D. W. O. Rogers, “The EGS4 code system”, SLAC 265, SLAC report Dec. 1985
- [8] P. Piot and Y.-E Sun, manuscript in preparation

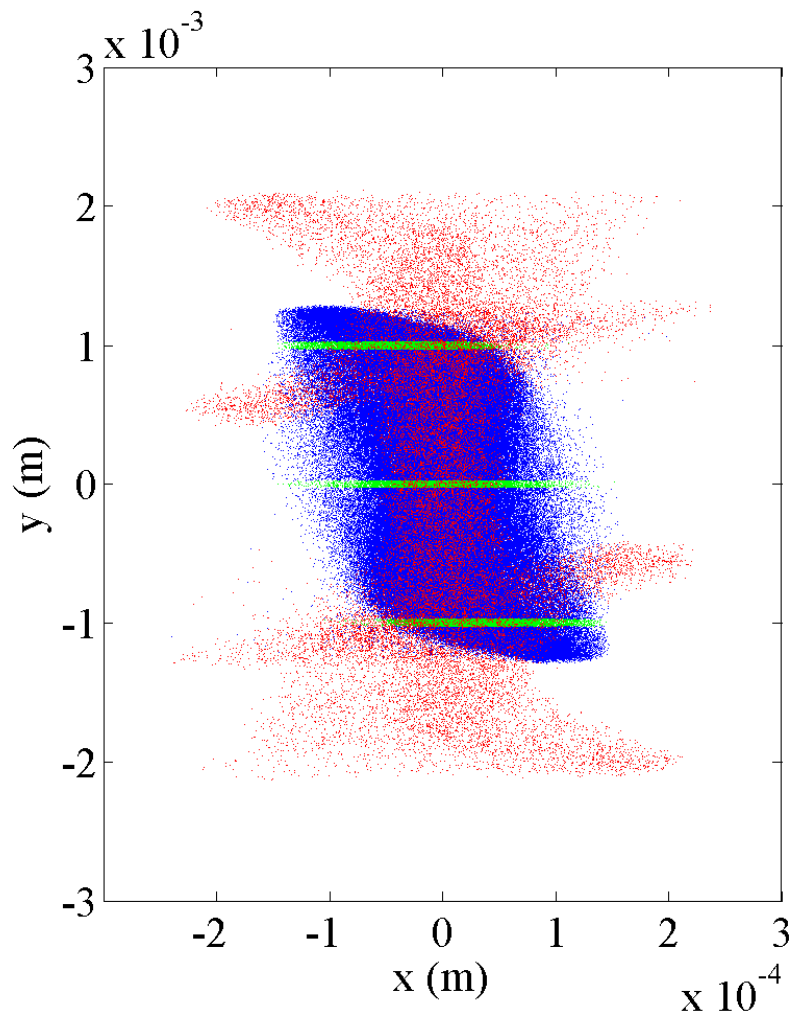


Figure 4: Beam on the viewer at $z = 5.61$ m (blue), horizontal slits inserted at the same location (green) and the beamlets what passed the slits at 40 cm drift away (red).

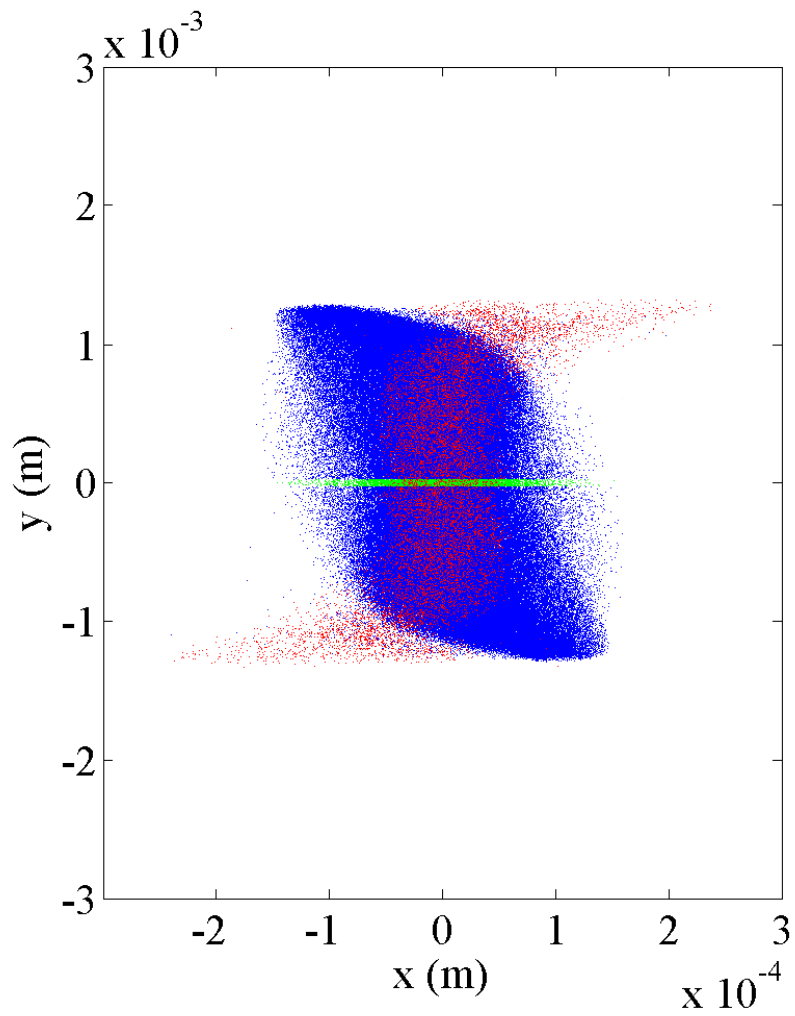


Figure 5: Beam on the viewer at $z = 5.61$ m (blue), a horizontal slit inserted at the same location (green) at the beam center and the beamlets what passed the slits at 40 cm drift away (red).

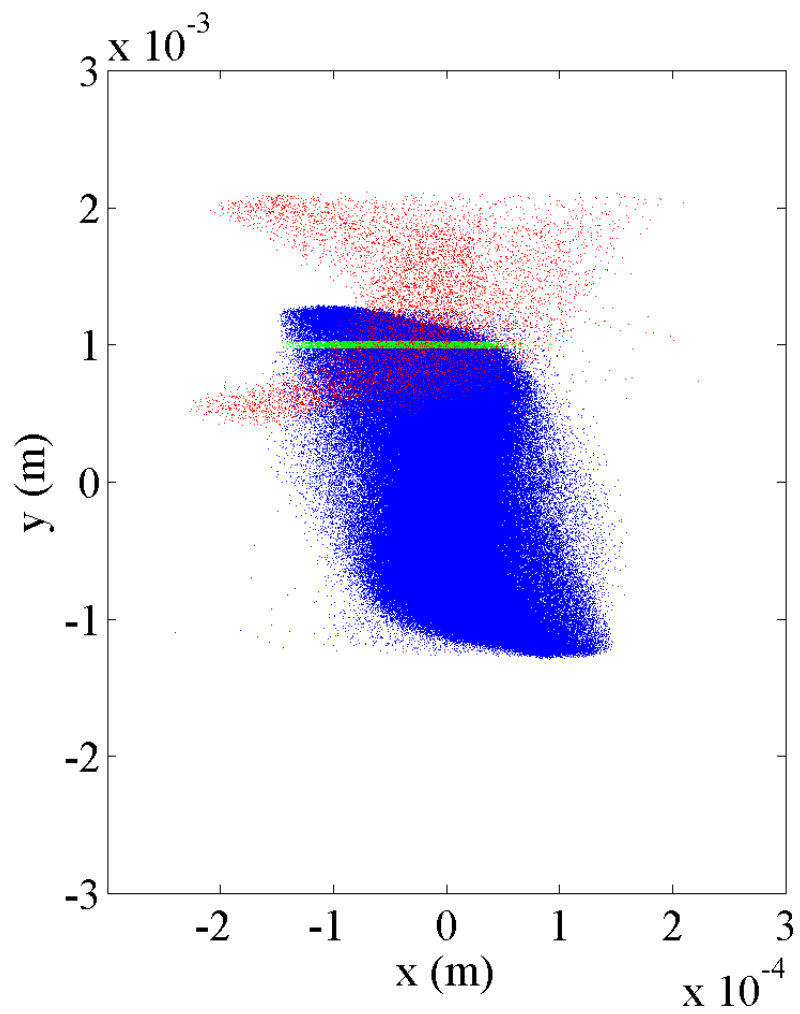


Figure 6: Beam on the viewer at $z = 5.61$ m (blue), horizontal slits inserted at the same location (green) at the top of the beam and the beamlets what passed the slits at 40 cm drift away (red).

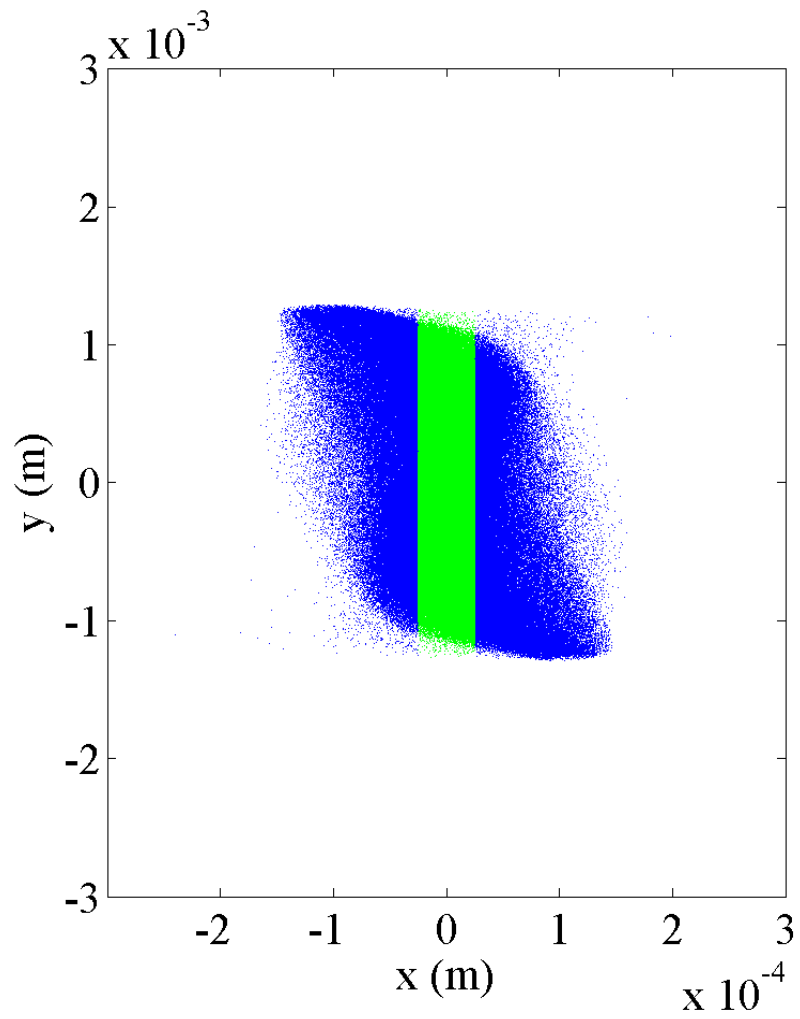


Figure 7: Beam on the viewer at $z = 5.61$ m (blue), a vertical inserted at the same location (green) at the center of the beam.

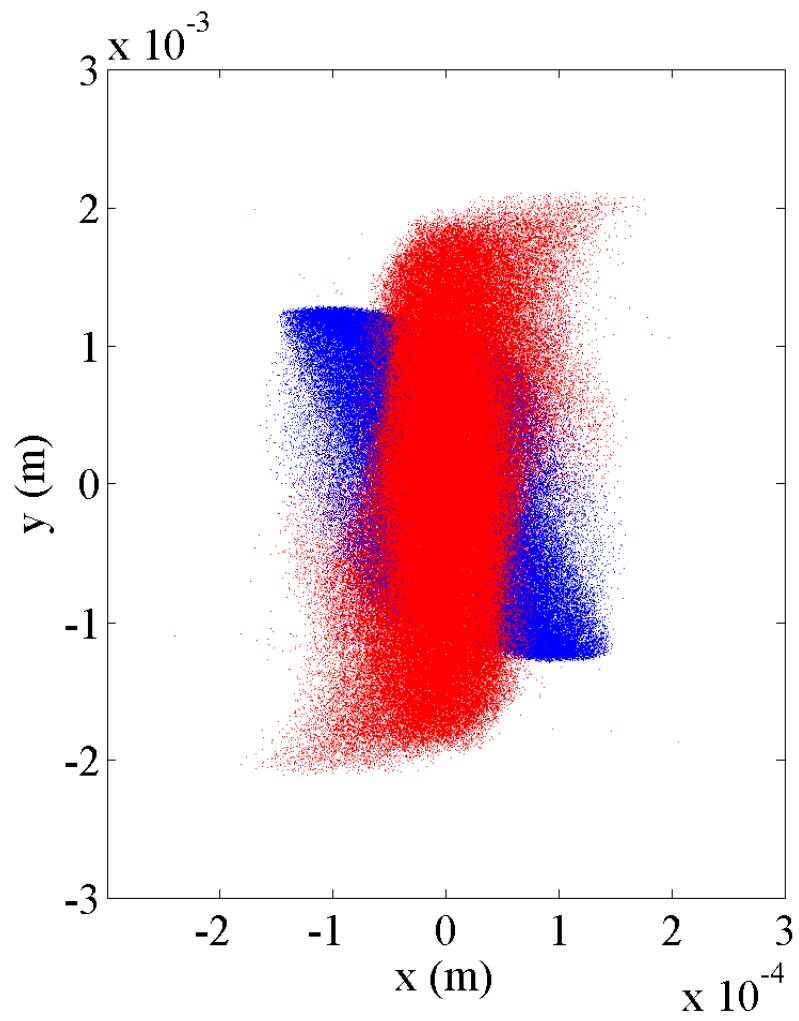


Figure 8: Beam on the viewer at $z = 5.61 \text{ m}$ (blue), the beamlets at 40 cm drift away (red).

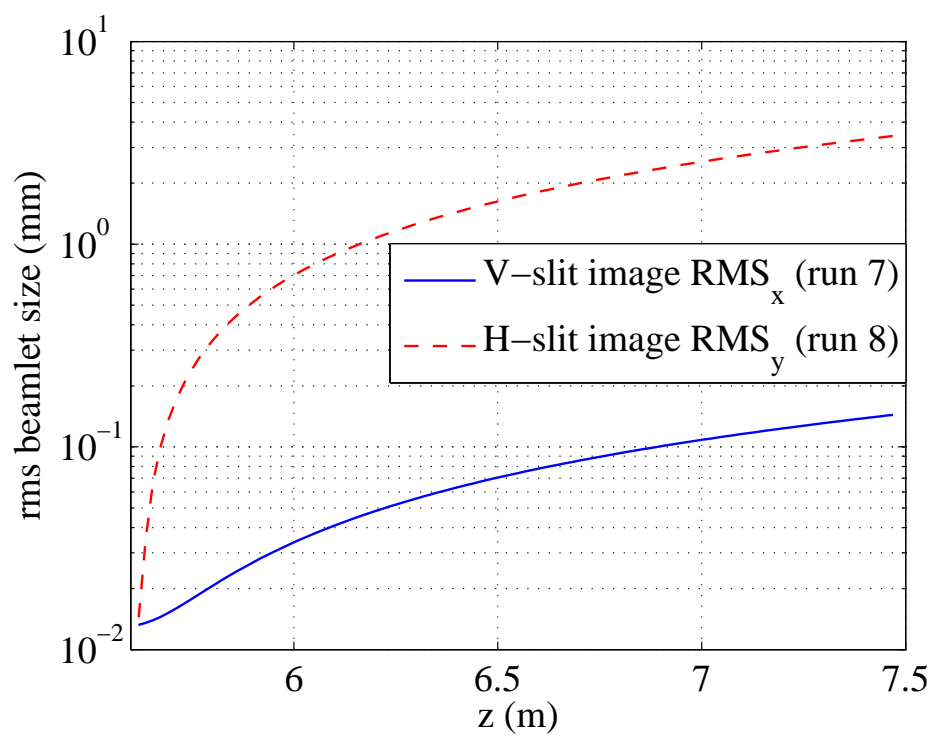


Figure 9: rms x of a vertical beamlet and rms y of a horizontal beamlet along the beam line.

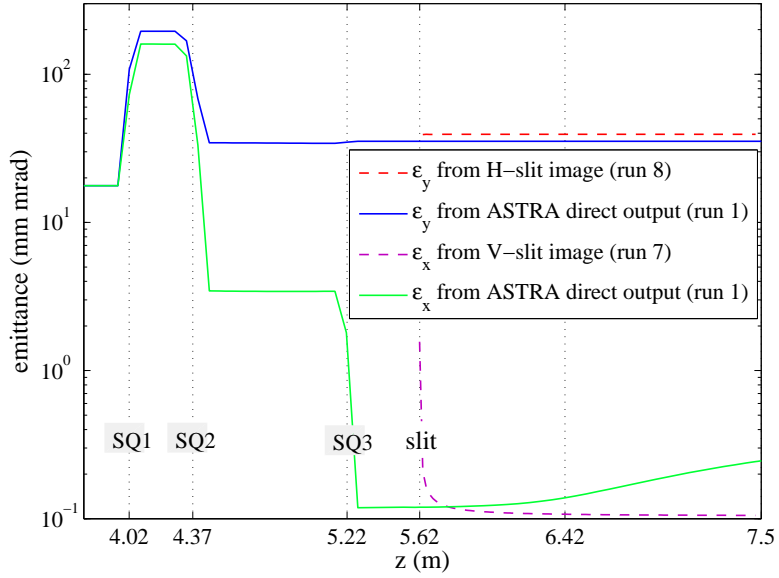


Figure 10: emittances measured from rms x of a vertical beamlet and rms y of a horizontal beamlet along the beam line.

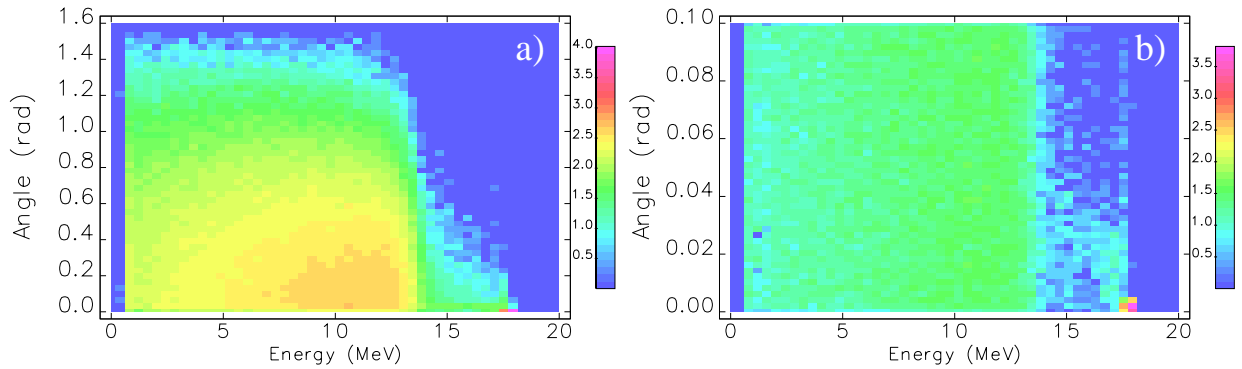


Figure 11: Energy-angle histogram of the electron distribution downstream of the slit mask. The calculations have been performed using the program `shower`. Plot b) is a zoom of plot a) for small angle.

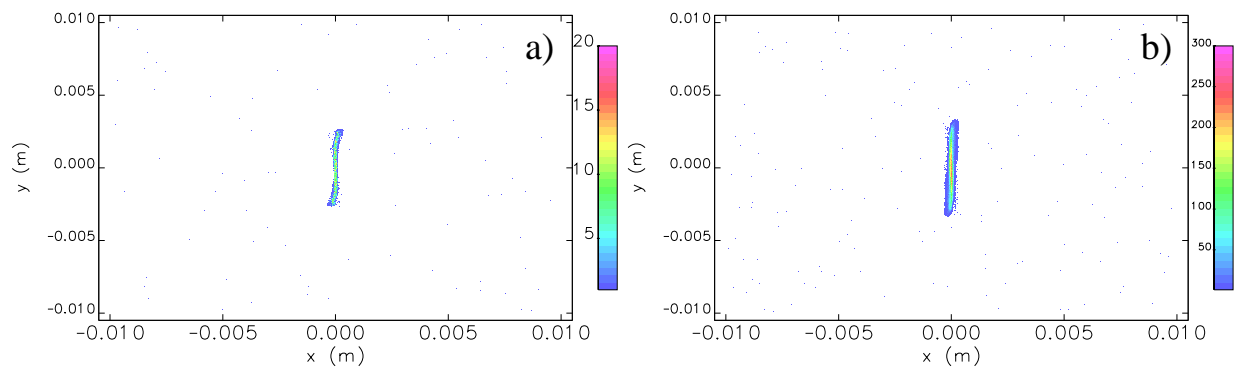


Figure 12: Simulated image for a beamlet going through an horizontal a) and vertical b) slits.

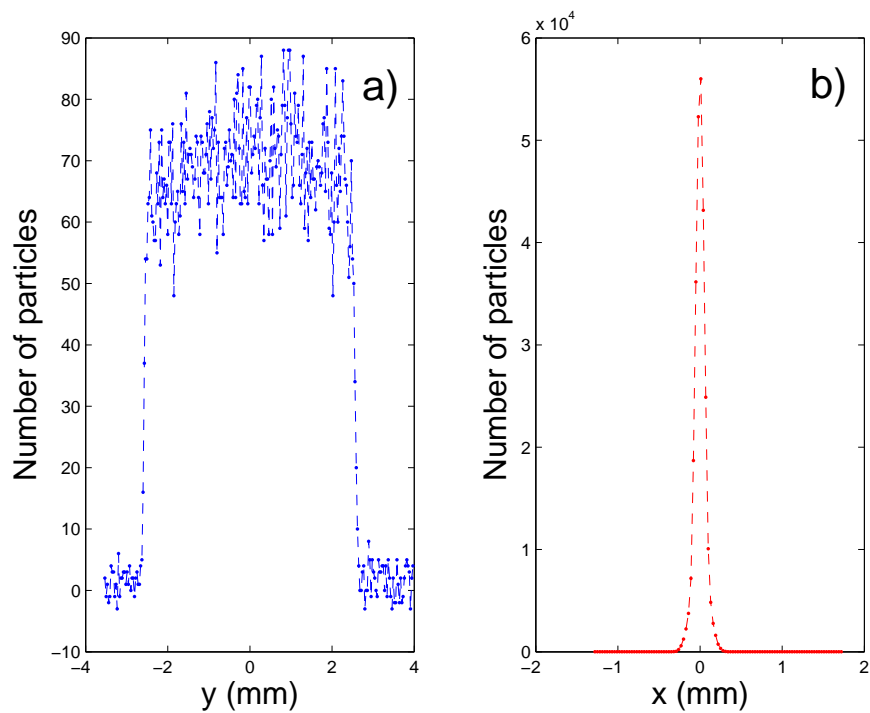


Figure 13: Simulated profile for a beamlet going through an horizontal a) and vertical b) slits. The profiles are directly computed as the projections along x and y axis of the image shown in Fig. 12.